ACTA MECHANICA SINICA (English Series), Vol.18, No.4, August 2002 ISSN 0567-7718
The Chinese Society of Theoretical and Applied Mechanics
Chinese Journal of Mechanics Press, Beijing, China
Allerton Press, INC., New York, U.S.A.

TWO BIFURCATION TRANSITION PROCESSES IN FLOATING HALF ZONE CONVECTION OF LARGER PRANDTL NUMBER FLUID*

Tang Zemei (唐泽眉) A Yan (阿 燕) Cao Zhonghua (曹重华) Hu Wenrui (胡文瑞)
(*National Microgravity Laboratory, CAS, Institute of Mechanics, CAS, Beijing* 100080, *China*)

ABSTRACT: Processes of the onset oscillation in the thermocapillary convection under the Earth's gravity are investigated by the numerical simulation and experiments in a floating half zone of large Prandtl number with different volume ratio. Both computational and experimental results show that the steady and axisymmetric convection turns to the oscillatory convection of $m = 1$ for the slender liquid bridge, and to the oscillatory convection before a steady and 3D asymmetric state for the case of a fat liquid bridge. It implies that, there are two critical Marangoni numbers related, respectively, to these two bifurcation transitions for the fat liquid bridge. The computational results agree with the results of ground-based experiments.

KEY WORDS: thermocapillary convection, microgravity fluid, numerical simulation, experiment

1 INTRODUCTION

The thermocapillary oscillatory convection in the floating half zone has been extensively studied since the middle of 1970s[1~3]. The process of onset oscillation and the mechanism of the thermocapillary oscillation are interesting due to its importance in both the basic research of microgravity fluid physics and its applications to materials processing. The theoretical studies on the onset of the oscillatory thermocapillary convection in the microgravity environment have been carried out in cases of the infinite planner layer[4], the infinite cylindrical liquid bridge[5] and the finite liquid bridge[6,7] for large or small Prandtl number fluid by using the method of linear stability analysis. The direct numerical simulations of a three-dimensional and unsteady model are applied to investigate the evolutionary process of onset oscillation, and give the flow field and temperature distribution of the thermocapillary convection[8~10]. A number of ground-based experiments of small-size liquid bridge have been conducted to study the onset of the oscillatory thermocapillary convection. The experiments discovered that the critical applied temperature difference ΔT_c depends sensitively on the volume ratio of the liquid bridge V/V_0, in addition to the aspect ratio $A = \ell/d$, and both of them are important critical geometrical parameters[11].

Received 18 March 2001, revised 30 October 2001
* The project supported by the National Natural Science Foundation of China (19789201) and the Ministry of Science and Technology of China (95-yu-34)

In the present paper, the transient process in a 10 cst silicon oil liquid bridge of 5 mm in diameter is investigated numerically and experimentally for two typical cases of a slender liquid bridge and a fat liquid bridge. The results of the numerical simulation agree well with those of experiments, and the experimental results give the transient process of two bifurcations in a fat liquid bridge for the first time.

2 NUMERICAL SIMULATION

2.1 The Physical Model

The numerical model is a floating half zone between two parallel and co-axial copper rods of 5 mm in diameter and 2.5 mm in height, and the liquid medium is 10 cst silicon oil ($Pr = 105.6$). The temperature T_2' at the upper rod is higher than temperature T_1' at the lower rod, and the temperature difference is $\Delta T' = T_2' - T_1'$. The configuration of the liquid bridge is shown in Fig.1, and the cylindrical coordinate system is adopted. The numerical simulation was performed for two typical cases of volume ratios V/V_0, where V and V_0 are, respectively, the volume of the liquid bridge and the volume of a cylinder with the same height and diameter. The direction of z-axis is opposite to the gravity vector. The free surface shape of the liquid bridge is determined by using the static condition of an isothermal liquid bridge under the earth's gravity, and is not changed during the computational process.

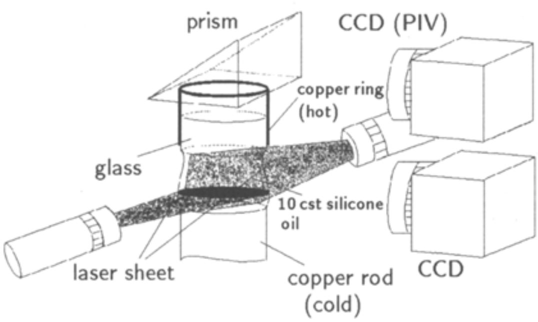

(a) Experimental model

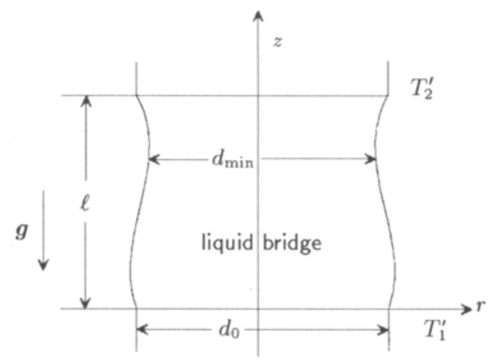

(b) Computational model

Fig.1 Schematic diagram of a liquid bridge

By using the Boussinesq approximation, the three-dimensional and time dependent Navier-Stokes equations and energy equation may be obtained. A constant temperature $T_*' = (T_1' + 100)$°C is adopted as the reference temperature in the present paper. The following dimensionless quantities are defined

$$
\begin{gathered}
r = \frac{r'}{\ell} \qquad z = \frac{z'}{\ell} \qquad u = \frac{u'}{U_r} \qquad v = \frac{v'}{U_r} \qquad w = \frac{w'}{U_r} \qquad t = \frac{t'}{\ell/U_r} \\
T = \frac{T'}{T_*' - T_1'} \qquad Re = \frac{U_r \ell}{\nu} \qquad Ma = \frac{U_r \ell}{\kappa} \qquad Gr = \frac{g\beta(T_*' - T_1')\ell^3}{\nu^2}
\end{gathered} \tag{2.1}
$$

where superscript prime denotes the dimensional quantities, for examples, (u', v', w') is the dimensional velocity vector, σ, β, ν, κ, ℓ, $\partial\sigma/\partial T$ and g are, respectively, the surface tension coefficient, the thermal expansion coefficient, the kinematic viscosity, the thermal diffusion coefficient, the height of the liquid bridge, the temperature gradient of the surface tension, and the earth's gravitational acceleration. The typical velocity $U_r = |\partial\sigma/\partial T|(T'_* - T'_1)/\rho\nu$ is obtained from the equilibrium condition of the tangential stress at the free surface. The Re, Gr, and Ma are, respectively, the Reynolds number, the Grashof number and the Marangoni number with the relationship $Ma = Re \cdot Pr$, where $Pr = \nu/\kappa$ is the Prandtl number.

The vectors of the stream function $\boldsymbol{\psi}$ and the vorticity $\boldsymbol{\omega}$ are introduced, respectively, in the dimensionless cylindrical coordinate system (r, θ, z) as follows[12]

$$\nabla \times \boldsymbol{\psi} = \boldsymbol{V} \tag{2.2}$$

$$\nabla \times \boldsymbol{V} = \boldsymbol{\omega} \tag{2.3}$$

Then, the dimensionless equations can be written as

$$\nabla \times \nabla \times \boldsymbol{\psi} = \boldsymbol{\omega} \tag{2.4}$$

$$\frac{\partial \boldsymbol{\omega}}{\partial t} + \boldsymbol{V} \cdot \nabla \boldsymbol{\omega} - \boldsymbol{\omega} \cdot \nabla \boldsymbol{V} = \frac{1}{Re}\left(\nabla^2 \boldsymbol{\omega} + \frac{\ell^2}{\rho\nu U_r} \nabla \times \boldsymbol{F}\right) \tag{2.5}$$

$$\frac{\partial T}{\partial t} + \boldsymbol{V} \cdot \nabla T = \frac{1}{Mr} \nabla^2 T \tag{2.6}$$

The boundary conditions are as follows

$$z = 0 \text{ and } z = 1: \quad \psi_r = \psi_\theta = 0 \qquad \frac{\partial \psi_z}{\partial z} = 0 \tag{2.7}$$

$$\omega_r = -\frac{\partial \nu}{\partial z} \qquad \omega_\theta = \frac{\partial u}{\partial z} \qquad \omega_z = 0 \tag{2.8}$$

at both the upper and lower boundaries $z = 0$ and $z = 1$

$$\begin{aligned} T(r, \theta, 0, t) &= 0 \\ T(r, \theta, 1, t) &= f(t) \end{aligned} \tag{2.9}$$

where dimensional α_T is a constant heating rate, and function $f(t) = \dfrac{\alpha_T t \ell}{(T'_* - T'_1)U_r}$. Furthermore

$$\psi_s = \psi_\theta = 0 \qquad \nabla \cdot \boldsymbol{\psi} = 0 \tag{2.10}$$

$$\omega_\theta = \frac{(1+f'^2)}{(1-f'^2)} \frac{\partial T}{\partial S} + \frac{2f'}{(1-f'^2)}\left(\frac{\partial u}{\partial r} - \frac{\partial w}{\partial z}\right) + 2\frac{\partial u}{\partial z} \tag{2.11}$$

$$\omega_z = \frac{(1+f'^2)^{1/2}}{r} \frac{\partial T}{\partial \phi} + 2\frac{\partial v}{\partial r} - f'\left(\omega_r + 2\frac{\partial v}{\partial z}\right) \tag{2.12}$$

$$\omega_r = \frac{1}{r}\frac{\partial w}{\partial \phi} - \frac{\partial v}{\partial z} \tag{2.13}$$

$$\frac{\partial T}{\partial n} = 0 \tag{2.14}$$

at the free surface of the liquid bridge, which is a rotational surface and symmetric to the z-axis, and can be described as $r = f(z)$.

2.2 Calculation Method

The hybrid method of fractional step[12] is used in the present paper. The numerical meshes are $12 \times 16 \times 12$ in r, θ, z directions, respectively, and the floating half zone is divided into 10 758 quadrilateral volume elements associated with 2 064 nodes, including 172 nodes in every layer. In order to consider the non-linear convective effects, the vorticity and energy equations are divided into the convection and the diffusion parts. The characteristic line method and the FEM method are used, respectively, for the convective terms and the diffusion operators.

The applied temperature difference $\Delta T'$ increases gradually from zero at the beginning, and the heating rate is $0.1\,^{\circ}\mathrm{C/s}$. The initial values of the temperature and the velocity are a constant and zero, respectively, in the liquid bridge.

The onset of thermocapillary convection is related to the grid adopted in the calculation. For checking the present numerical program, the thermocapillary convection calculated for a cylindrical liquid bridge with $g = 0$ and $\ell/d_0 = 10$ is compared with those obtained from linear stability analysis for infinite length, cylindrical liquid bridge[5] and calculated by using three-dimensional axisymmetric program. The results are in a quite good agreement, apart from a maximum error 14% at the meshes near the free surface. It shows the core velocity profile for buoyancy convection in a horizontal cylinder of the present calculation agrees well with the results of Bejan et al.[13]. The calculated results for different grids are shown in the following Table 1.

Table 1 The calculated results for different grids

Grid ($n_r \times n_\theta \times n_z$)	$\Delta T'_{c1}/^{\circ}\mathrm{C}$	$U_{\max}$ $\Delta T = 4^{\circ}\mathrm{C}$, $z/\ell = 0.55$	T $\Delta T' = 4^{\circ}\mathrm{C}$, $z/\ell = 0.55$
$12 \times 16 \times 12$	5.17	-5.019×10^{-2}	0.731
$16 \times 24 \times 16$	4.69	-5.270×10^{-2}	0.715
$12 \times 24 \times 12$	3.18	–	–

The same unstable modes of thermocapillary convection were shown qualitatively in the calculation for three different grids. The relationship between critical temperature difference and volume ratio calculated by using the present program agrees also well with experimental results[11].

2.3 Calculation Results

It is usually considered that the steady and axisymmetric thermocapillary convection becomes the oscillatory convection when the applied temperature difference is larger than a critical one in the case of large Prandtl number liquid bridge. The linear stability analyses[7] and the three-dimensional numerical simulation[8~10] demonstrated that the steady and axisymmetric thermocapillary convection turns to the oscillatory convection via the steady and axial asymmetric convection in the case of small Prandtl number fluid. The similar conclusion holds in case of a fat liquid bridge with larger Prandtl number[11,14].

The quantities $\delta_v = (V_{\max} - V_{\min})/U_{\max}$ and $\delta_T = (T'_{\max} - T'_{\min})/\Delta T'$ were used to describe the variations of the velocity and temperature fields in the transition process during increasing of the applied temperature difference[11]. $V_{\max}$, $V_{\min}$, $T'_{\max}$ and $T'_{\min}$ are the maximum and the minimum values of the azimuthal velocity components and the temperatures at the free boundary of the horizontal cross-sections with $z/\ell = 0.55$, and $U_{\max}$ is the maximum velocity in the liquid bridge corresponding to the applied temperature difference $\Delta T'$.

For studying the case of two-bifurcation transition, the temperature difference relating to the condition $\delta_v/2 = 1\%$ is defined as the first critical temperature differences $\Delta T'_{c1}$. The steady and axisymmetric thermocapillary convection turns to the steady and axial asymmetric convection if $\Delta T'$ is a bit larger than $\Delta T'_{c1}$. The second critical temperature difference is $\Delta T'_{c2}$, which is defined as the onset of temperature oscillatory in a thermocapillary convection. In the case of oscillatory convection, the applied temperature difference is larger than $\Delta T'_{c2}$. $\Delta T'_{c1}$ and $\Delta T'_{c2}$ depend on the volume ratio of liquid bridge V/V_0. The temperature evolutionary processes of four points at the boundary of horizontal section at $z/\ell = 0.55$ are shown in Fig.2 for the case of the slender liquid bridge $V/V_0 = 0.8$ (Fig.2(a)) and a fat liquid bridge 0.985 (Fig.2(b)). It shows that the steady and axisymmetric convection turns directly to the oscillatory one for a slender liquid bridge $V/V_0 = 0.8$, and the oscillation mode is $m = 1$. In this case, there is only one bifurcation relating to the onset of oscillation, $\Delta T'_{c1} = 20.118°\text{C}$, $Re_c = 32.275$ and $Ma_c = 3\,408$. For the case of the fat liquid bridge $V/V_0 = 0.985$, the first critical temperature difference $\Delta T'_{c1} = 5.17°\text{C}$ and the second critical temperature difference $\Delta T'_{c2} = 41°\text{C}$. The related Reynolds numbers are 8.3 and 65.78, and Marangoni numbers are 876 and 6 946. The velocities of four points are separated before oscillation and the oscillation mode is $m = 2$. If the applied temperature difference is fixed at 30°C, which is higher than $\Delta T'_{c1}$ and lower than $\Delta T'_{c2}$, for the fat liquid bridge $V/V_0 = 0.985$, the azimuthal velocities are different and unvaried with time at four boundary points. The steady and axial asymmetric temperature distribution and flow field in the horizontal cross section $z/\ell = 0.5$ are observed in upper and middle of Fig.3 and the relating normal flow field is shown in the lower of Fig.3, which looks like a symmetric one. The convection is steady and asymmetric. It means that the steady and axi-symmetric thermocapillary convection turns to the steady and axial asymmetric convection for the fat liquid bridge ($V/V_0 = 0.985$) when $\Delta T'_{c2} > \Delta T' > \Delta T'_{c1}$.

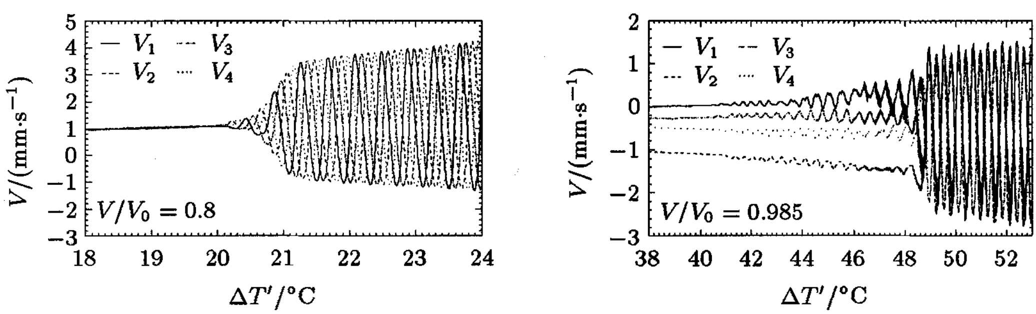

(a) $V/V_0 = 0.80$ (b) $V/V_0 = 0.985$

Fig.2 The transient feature of azimuthal velocity

Furthermore, the steady and non-axisymmetric convection turns to the oscillatory convection if $\Delta T' > \Delta T'_{c2}$. The temperature profiles in one period in a horizontal cross-section at $z/\ell = 0.5$ are given in Fig.4 for a fat liquid bridge of $V/V_0 = 0.985$ ($m = 2$). The configurations rotate at a frequency the same as that of the related flow-field patterns, however, the fluid particles do not rotate. Same rotating patterns of the azimuthal velocity are observed by

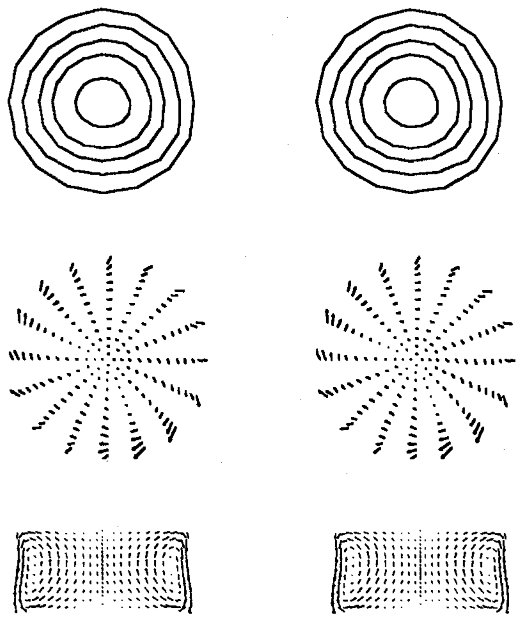

(a) $t = 326.18\,\text{s}$ (b) $t = 346.57\,\text{s}$

Fig.3 The temperature distribution (upper) and azimuthal velocity field (middle) and velocity (lower) in a vertical cross section for a fixed temperature difference $\Delta T' = 30°\text{C}$ ($V/V_0 = 0.985$)

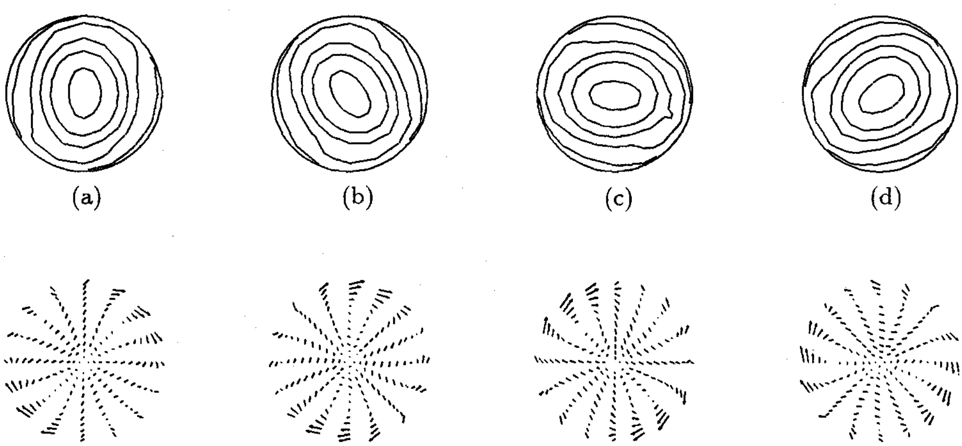

(a) (b) (c) (d)

Fig.4 The evolutions of temperature distribution (upper) and azimuthal velocity field (lower) in the oscillatory convection ($V/V_0 = 0.985$, $z = 0.5$)

the ground-based experiment[15]. The rotating patterns of temperature and flow field nearly keep their configuration during the rotating process, and the results disagree with that of the paper[16], which suggested that the fluid rotates together with the pattern.

The onset process of the fat liquid bridge is quite different from that of the slender one. The onset processes of oscillatory convection for both liquid bridges are described by

δ_v as shown in Fig.5. For both liquid bridges, the thermocapillary convection is steady if the applied temperature difference $\Delta T'$ are smaller than the critical value $\Delta T'_{c1}$ and the velocity field and temperature distribution are axisymmetric. Therefore, δ_v and δ_T are small and close to zero. In the case of slender liquid bridge, for example, $V/V_0 = 0.8$, the steady and axisymmetric convection turns to the three-dimensional and time dependent oscillatory convection in a short time period, and the value of δ_v increases rapidly. The case of slender liquid bridge was discussed in detail in [11]. For the case of the fat liquid bridge $V/V_0 = 0.985$, the oscillatory velocity is excited in a longer period during increasing of the applied temperature difference.

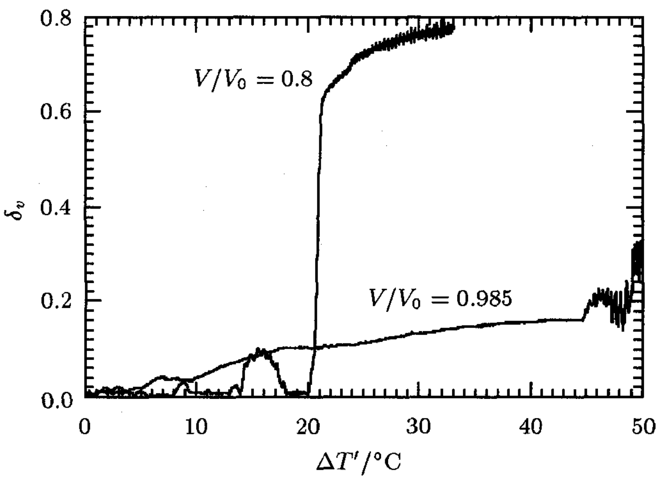

Fig.5 The transient process described by the parameters δ_v and δ_T

3 EXPERIMENTS

3.1 Experimental Condition

The liquid bridge adopted in the experiment has the same geometric configuration and physical parameters as those in the calculation. The liquid bridge of 10 cst silicone oil is floated in the gap between two co-axial disks with the same diameter $d_0 = 5$ mm. The lower disk consists of a copper. The upper disk is transparent for observation of the flow pattern in the horizontal cross-section, and consists of transparent K9 glass disk fitted well by a surrounding copper heater, which does not in contact with the liquid bridge and is around the glass disk as shown in Fig.1(a). The thickness of the circular glass disk is $h = 5$ mm.

The temperatures are measured by thermocouples at both sides of the solid disks. A PID-controller (EUROTHERM 904 controller) is used to control the heating rate, and the temperature difference between the upper disk boundary at free surface and the lower disk. A Flowmap PIV system is used to measure quantitatively the velocity distribution of the flow field in a horizontal cross-section of the liquid bridge. The hollow glass spheres of 10 μm in mean diameter are suspended in the liquid bridge as particle tracers. The density $\rho = 1.1\,\mathrm{g/cm^3}$ of tracer particles is close to the density $\rho = 0.94\,\mathrm{g/cm^3}$ of 10 cst silicone oil. A horizontal cross-section of the liquid bridge is illuminated by a light-sheet of 0.3 mm thickness of an argon ion laser with power of 1.0 W. Another light-sheet of a He-Ne laser is applied vertically for the horizontal cross-section measurement, with the laser power of

5 mW. An 80C42 Double Image 700 camera is used to record images in the PIV system. The illumination system and camera are controlled automatically by a synchronization board in the PIV 2 000 processor, which processes images into vector results in real-time. Vector map acquisition at a frequency of 15 Hz makes it possible to distinguish whether the flow field is in a stationary state in a liquid bridge.

3.2 Transition Process for Fat Liquid Bridge

The temperature difference $\Delta T'$ between two ends of the liquid bridge is applied, linearly increasing with time. The heating rate of the experiment is 4.0°C/min. The evolution of thermocapillary convection is observed during the increasing of the temperature difference. In this process, the velocity distribution in the horizontal cross section at $z/\ell = 0.25$ of the liquid bridge is measured by using PIV in real time, and the successive vector maps are captured at time intervals of 66 ms.

The comparison of successive frames of velocity field can indicate clearly the process of symmetry breaking and the onset of oscillation. It is observed that, the steady and axis-symmetric flow turns to a steady and asymmetric flow for a fat liquid bridge with small aspect ratio. Figure 6 displays a typical example of asymmetric, three-dimensional stationary flow configuration in a fat liquid bridge of aspect ratio $A = 0.5$ and volume ratio $V/V_0 = 1.1$. When the applied temperature difference increases to and keeps at $\Delta T' = 22$°C, which is higher than the first critical value for onset of the asymmetric convection and lower than the second critical value for onset of oscillation, the velocity distributions are asymmetric and steady. Figures 6(a) and 6(b) show two velocity distributions in the same section $z/\ell = 0.25$ but with 120 s of time duration, and the flow pattern keeps nearly the same. The time evolution of the azimuthal velocity at same radius $r = 2.2$ mm but different azimuthal angles $\theta = 140°$ and $\theta = 230°$ in a cross-section $z/\ell = 0.25$ was shown in Fig.7 in case of an applied temperature difference $\Delta T' = 20.4$°C. It shows that the asymmetric velocity field is independent of time.

In order to verify the calibration and validation of the experimental technique, the

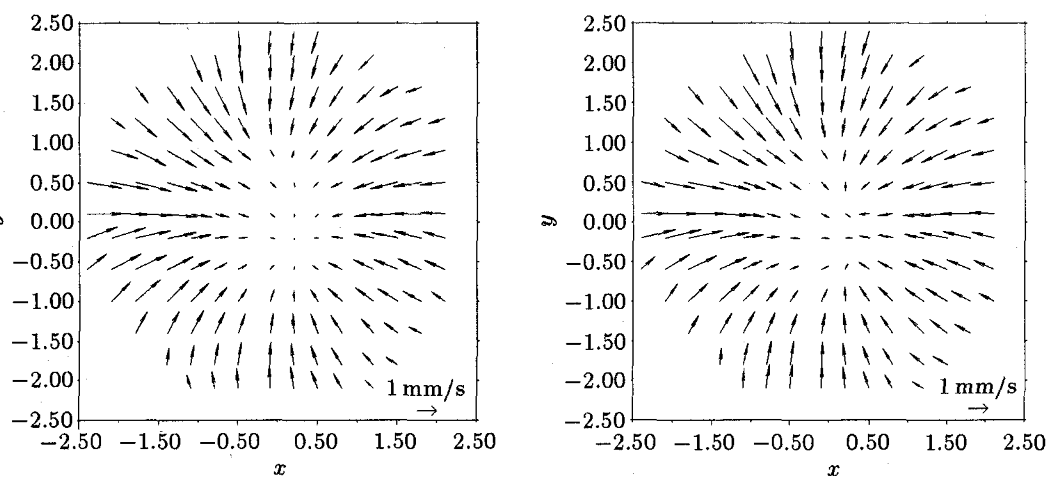

(a) $t = t_0$ (b) $t = t_0 + 120$ s

Fig.6 The steady and asymmetric distribution of velocity in a horizontal cross-section ($z/\ell = 0.25$) of a fat liquid bridge ($V/V_0 = 1.1$) at different time when temperature difference $\Delta T' = 22$°C

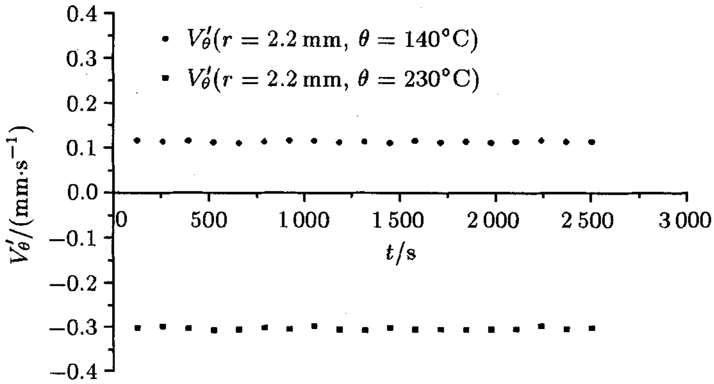

Fig.7 A graph for the variation of azimuthal velocity with time at two fixed points ($r = 2.2\,\text{mm}$, $\theta = 140°$ and $\theta = 230°$, $z/\ell = 0.25$) of flow field in a horizontal cross-section of liquid bridge when temperature difference $\Delta T' = 20.4°\text{C}$

velocities of a model, whose input parameters are the direction and magnitude of the flow at a fixed point in a liquid bridge, were measured as reported in Ref.[15]. The velocity measurement accuracy is better than 5%. In the present experiment, the measured radial velocity is much larger than the azimuthal velocity. By using the PIV method, it should be remembered that the accuracy is in an absolute value, and a larger measurement error may appear in case of a small velocity value than that of a large velocity value, although the accuracy is generally expressed as a percentage of the measured full-scale velocity. The radial component of velocity can be measured with much better accuracy than the azimuthal velocity component.

To estimate the asymmetric degree of velocity distribution, a characteristic velocity $\Delta V'_\theta = |V'_{\theta\max} - V'_{\theta\min}|$ is introduced, where $V'_{\theta\max}$ and $V'_{\theta\min}$ are, respectively, the maximum and minimum value of azimuthal velocity at radius $r = (2.2 \pm 0.05)\,\text{mm}$ in a cross-section $z/\ell = 0.25$. Figure 8 summarizes the experimental results of asymmetric degree $\Delta V'_\theta$ depending on the applied temperature difference in case of a fat liquid bridge $V/V_0 = 1.1$ (circle marks), and case of a slender liquid bridge $V/V_0 = 0.8$ (square marks). It could be seen that $\Delta V'_\theta$ keeps a lower constant and then has a sharp increment at $\Delta T' \cong 23°\text{C}$ related to the onset of oscillation during the increasing of the applied temperature difference for the case of volume ratio $V/V_0 = 0.8$. However, $\Delta V'_\theta$ keeps constant when applied temperature difference $\Delta T' < 13°\text{C}$, and then increases gradually with the applied temperature difference ΔT before the onset of oscillation for the case of volume ratio $V/V_0 = 1.1$. The asymmetric degrees of velocity distributions $\Delta V'_\theta$ remain nearly $\Delta V'_\theta = 0.21 \sim 0.25\,\text{mm/s}$ for different liquid bridge volumes when the temperature differences are lower. $\Delta V'_\theta$ is considered to be caused by the system errors of the experiment.

For the case of $V/V_0 = 1.1$, the onset of the first bifurcation may be defined by the moment $\Delta V'_\theta = 0.25\,\text{mm/s}$, and it gives

$$\Delta T'_{c1} = 13°\text{C} \tag{3.1}$$

This value relates to the transition from the steady and axisymmetric convection to the steady and asymmetric convection. The critical value of the applied temperature difference

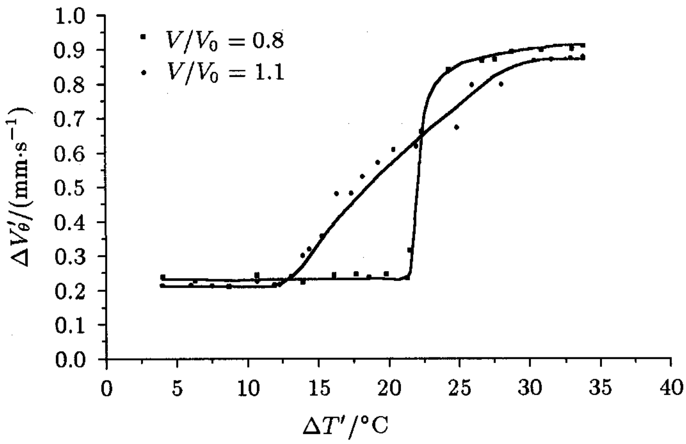

Fig.8 The relationship between asymmetric degree $\Delta V'_\theta$ and temperature difference $\Delta T'$ for the different volume ratio $V/V_0 = 0.8$ and $V/V_0 = 1.1$

related with onset of oscillatory may be given, experimentally, as

$$\Delta T'_{c2} = 30.4°\mathrm{C} \tag{3.2}$$

The sequence of flow pattern in a horizontal cross-sections at $z/\ell = 0.60$ in one period of oscillation for the case $V/V_0 = 1.1$ is given in Fig.9 for $\Delta T' = 32°\mathrm{C}$. In this case, the oscillatory frequency is 0.92 Hz. The results show that, the flow patterns appear as the asymmetric mode $m = 2$, and the oscillatory configurations are related to a pulsating instability. The oscillatory flow is characterized by a standing wave.

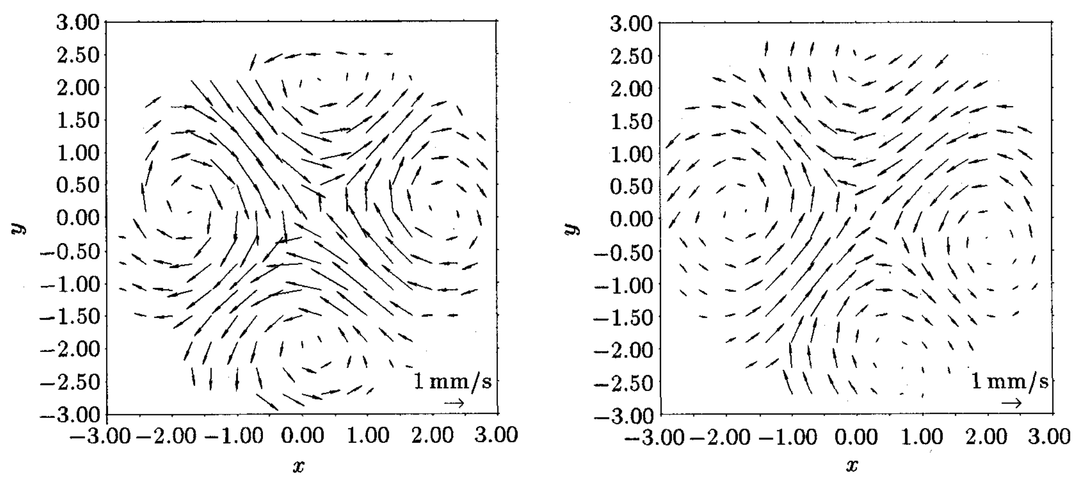

Fig.9 A sequence of flow pattern in the horizontal cross-section ($z/\ell = 0.6$) in one oscillatory period in a fat liquid bridge. The time step is one half of the oscillatory period in case of $V/V_0 = 1.1$ and $\Delta T' = 32°\mathrm{C}$

3.3 Transition Process for Slender Liquid Bridge

It is observed that axial-symmetry is lost at the same moment as the onset of oscillation in a slender liquid bridge. The velocity fields measured in the cross-section $z/\ell = 0.25$

for the case $V/V_0 = 0.8$ show that, once the motion is asymmetric, azimuthal velocity starts to oscillate. The transition point between subcritical axisymmetric and supercritical asymmetric state is determined experimentally for the case $V/V_0 = 0.8$ as

$$\Delta T'_{c1} = \Delta T'_{c2} = 21.5°\mathrm{C} \tag{3.3}$$

Figure 10 shows the sequence of flow pattern in one period of oscillation of the horizontal cross-sections at $z/\ell = 0.60$ for the case $V/V_0 = 0.8$ when $\Delta T' = 23°\mathrm{C}$. In this case, the oscillatory frequency is 0.67 Hz. The results show that, the flow patterns appear as a mode $m = 1$, and oscillation configurations are related to a rotating instability. The oscillatory flow is characterized by a traveling wave.

The tracer particle accumulation structures (PAS) the same as Ref.[17] occurred before the onset of oscillation in our experiments. Some regions may become tracer-free after some

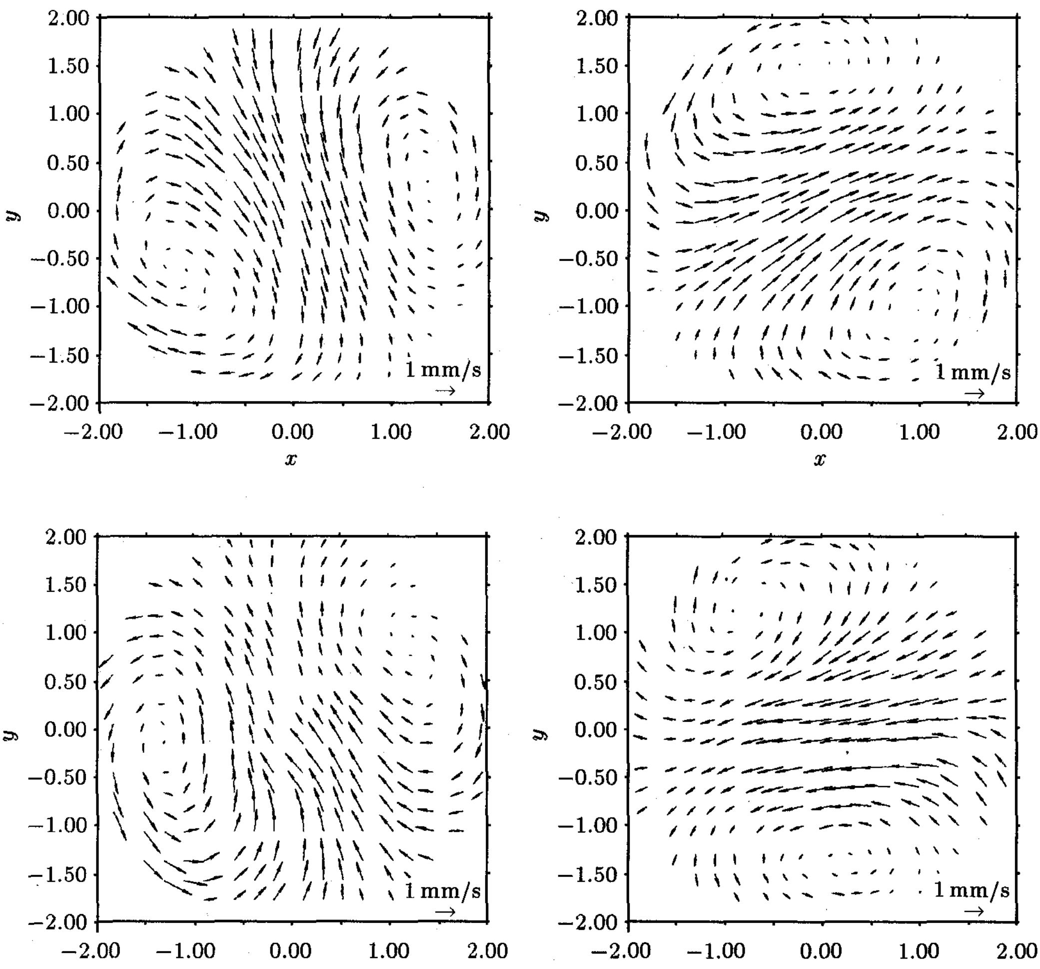

Fig.10 A sequence of flow pattern in the horizontal cross-section ($z/\ell = 0.6$) in one oscillatory period in a slender liquid bridge. The time step is one-fourth of the oscillatory period in case of $V/V_0 = 0.8$ and $\Delta T' = 23°\mathrm{C}$

time, where no flow velocity can be measured any more. It is difficult to measure the velocity distributions in a horizontal cross-section of the liquid bridge in this case. So only the azimuthal velocity distributions of two typical examples for the case $V/V_0 = 0.8$ and $V/V_0 = 1.1$ are selected to make a comparison of asymmetric degree.

3.4 On Transition Process

The experimental results have shown that two bifurcation transitions were observed in a fat liquid bridge of large Prandtl number: firstly from steady and axial-symmetric convection to the steady and asymmetrical, and then to the oscillatory convection at a larger temperature difference. The oscillation convection appears as the mode $m = 2$, and as a "pulsating" flow state for the case of $A = \ell/d_0 = 0.5$, $V/V_0 = 1.1$. Two bifurcation transitions are not found in the slender liquid bridges of 10 cst silicone oil in our experiments, and only one transition from steady and axial-symmetric state to an asymmetric and oscillatory state of thermocapillary convection is observed for the case of $A = \ell/d_0 = 0.5$, $V/V_0 = 0.8$. The oscillatory convection appears as the mode $m = 1$ and the "rotating" flow state.

There are two main reasons about the selection of the section at $z/\ell = 0.25$ where the velocity distributions are measured. On the one hand, asymmetry is obvious in this section for the case $V/V_0 = 1.1$ when $\Delta T' > \Delta T'_{c1}$. On the other hand, there are less tracer-free regions in this section than in other sections. The flow is recorded from the top through the glass disk. The velocities close to free surface of the liquid bridge can not be measured in this section ($z/\ell = 0.25$) because the area of this section is larger than that of glass disk. The azimuthal mode of steady and three-dimensional convection in the liquid bridge of 10 cst silicone oil for this case could not be determined in this experiment.

4 COMPARISON OF THEORETICAL AND EXPERIMENTAL RESULTS

The onset of oscillatory thermocapillary convection under the earth's gravity was investigated by both the numerical simulation and experimental methods. The liquid bridge adopted in the experiment has the same geometric configuration and physical parameters as those in the numerical simulation. The calculated results are compared with the experimental ones for cases of a fat liquid bridge of $V/V_0 = 0.985$ and a slender liquid bridge of $V/V_0 = 0.8$ in Table 2.

Table 2 Comparison of the numerical simulation results and the experimental results

	Experimental results		Computational results	
height of liquid bridge	2.5 mm		2.5 mm	
diameter of liquid bridge	5.0 mm		5.0 mm	
medium	10 cst silicon oil		10 cst silicon oil	
volume ratios	0.8	0.985	0.8	0.985
first critical temperature difference	21.5°C	10.5°C	20.118°C	5.17°C
second critical temperature difference	21.5°C	34.6°C	20.118°C	41°C
first critical Renolds number	34.492	16.8	32.275	8.3
second critical Renolds number	34.492	55.5	32.275	65.78
first critical Marangoni number	3642	1779	3408	876
second critical Marangoni number	3642	5861	3408	6946

Both results for the case of a slender liquid bridge are in good agreement, and the critical Marangoni number is 3 642 for experiment and 3 604 for numerical simulation. The relative difference is only 1 percentage. For the case of fat liquid bridge, the second critical Marangoni number is 5 861 for experiment and 6 946 for numerical simulation, and the relative difference is 17%. Both results are in a reasonable agreement. The first critical Marangoni number for a fat liquid bridge is 1 779 for experiment, which is about twice as the one of only 876 for numerical simulation. However, both the experiment and the numerical simulation proved the process of two bifurcation transitions in a fat liquid bridge,

5 CONCLUSION AND DISCUSSION

The three-dimensional steady and asymmetric distributions of the flow field and the temperature field exist before the onset of oscillatory flow, obtained by the three dimensional and unsteady numerical simulations[8~10] and the linear stability analysis[7] in case of the small Prandtl number liquid bridge. Frank and Schwabe[18] observed also the time-independent and three-dimensional flow state in their experiments of thermocapillary convection of liquid bridge with Prandtl number $= 7, 49, 65$, and conjectured that the broken symmetry convection was probably caused by a hydrodynamical instability.

By using the linear instability analysis, Chen and Hu pointed that the steady and axisymmetric thermocapillary convection can have an instability mode of a steady and axial asymmetric state for a fat liquid bridge of large Prandtl number[19]. The computational results of liquid bridge under microgravity are consistent with the results of the present paper[14]. In the present paper, the flow state with steady and axial asymmetry was observed clearly for a typical fat bridge $V/V_0 = 0.985$ if the applied temperature difference $\Delta T' = 30°\mathrm{C}$ is fixed. It means that there is a transition from steady and axisymmetric convection to the steady asymmetric convection for the fat liquid bridge with large Prandtl number. These results imply that, the geometrical parameter V/V_0 is not only a sensitive critical parameter for the onset of oscillatory thermocapillary convection, but also is an important factor for studying the transition mechanism of thermocapillary convection even for the case of large Prandtl number fluid. The numerical results are compared with the ground-based experiments[14], and both results are in a reasonable agreement.

The results of the present paper only give an example, and show that there are two bifurcation transitions in a liquid bridge of large Prandtl number. The conclusion of the present paper agrees with that obtained by the linear instability analysis by Chen and Hu[19], and that in the microgravity environment[11]. The two bifurcation transitions exist not only in the liquid bridge of small Prandtl number, but also in the liquid bridge of larger Prandtl number.

Further studies of both numerical simulations and experiments should be carried out on the effect of liquid bridge volume on the transition process, which is related to the new mechanism for the onset of oscillatory convection in the floating half zone.

REFERENCES

1 Chun CH, West W. Experiments on the transition from the steady to the oscillatory Marangoni-convection of a floating zone under reduced gravity effect. *Acta Astronautica*, 1979, 6(9): 1073~1082

2 Preisser F, Schwabe D, Scharmm A. Steady and thermocapillary convection in liquid columns with free cylindrical surface. *J Fluid Mechanics*, 1983, 126: 545~567

3 Cao ZH, You HT, Tang ZM, et al. Experimental investigation of thermocapillary convection in half floating zone. *Adv Space Res*, 1991, 11(7): 229~232

4 Smith MK, Davis SH. Instabilities of dynamic thermocapillary liquid layers, Part I: Convective instabilities. *J Fluid Mech*, 1983, 132: 119~144

5 Xu JJ, Davis SH. Convective thermocapillary instability in liquid bridges. *Phys Fluid*, 1984, 27(5): 1102~1107

6 Wanschura M, Shevtsova VM, Kuhlmann HC, et al. Convective instability mechanisms in thermocapillary liquid bridges. *J Phys Fluids*, 1995, 7(5): 912~925

7 Chen QS, Hu WR. Effect of liquid bridge volume on instability of floating half zone convection. *International J Heat and Mass Transfer*, 1998, 41(5): 825~837

8 Rupp R, Muller G, Neumann G. Three-dimensional time dependent modeling of the Marangoni convection in zone melting configurations for gas. *J Crystal Growth*, 1989, 97(1): 34~41

9 Levenstam M, Amberg G. Hydrodynamical instabilities of thermocapillary flow in a half-zone. *J Fluid Mech*, 1995, 297: 357~372

10 Savino R, Monti R. Oscillatory Marangoni convection in cylindrical liquid bridge. *Phys Fluids*, 1996, 8(1): 2906~2921

11 Tang ZM, Hu RW. Influence of liquid bridge volume on the onset of oscillation in floating half-zone convection III: Three-dimensional model. *J Crystal Growth*, 1999, 207(3): 239~246

12 Wu JH. A hybrid method of fractional steps with L_∞——stability for numerical modelling of aquatic environments. *Research and Development on Hydrodynamics*, 1985(1): 27~36

13 Bejan A, Tien CL. Fully developed natural counterflow in a long horizontal pipe with different end temperatures. *Int J Heat Mass Transfer*, 1978, 21(6): 701~708

14 Tang ZM, Hu WR, Imaishi N. Two bifurcation transitions of the floating half zone convection in a fat liquid bridge of large *Pr* number. *Int Journal of Heat and Mass Transfer*, 2001, 44(7): 1299~1307

15 Ar Y, Tang ZM, Han JH, et al. The measurement of azimuthal velocity field for oscillatory thermocapillary convection. *Microgr Sci and Tech*, 1998, 10(3): 129~135

16 Lee J, Lee DJ, Lee JH. On the mechanism of oscillation in a simulated floating zone. *J Crystal Growth*, 1955, 152(4): 341~346

17 Schwabe D, Hintz P, Frank S. New features of thermocapillary convection infloating zones revealed by tracer particle accumulation structures (PAS). *Microgravity Sci Technol*, 1996, 9(3): 163~168

18 Frank S, Schwabe D. Temporal and spatial elements of thermocapillary convection in floating zones. *Experiment in Fluids*, 1997, 23(3): 234~251

19 Chen QS, Hu WR. Instability from steady and axial-symmetric to steady and asymmetric floating half zone convection in a fat liquid bridge of large *Pr* number. *Chinese Physics Letter*, 1999, 16(11): 822~823